Applied Mechanics and Materials
ISSN: 1662-7482, Vol. 876, pp 57-63
doi:10.4028/www.scientific.net/AMM.876.57

Submitted: 2017-06-25
Revised: 2017-09-06
Accepted: 2017-09-06
Online: 2018-02-01

Preparation and Characterization of Advanced PtRu/$Ti_{0.7}Mo_{0.7}O_2$ Catalysts for Direct Methanol Fuel Cells

Van Thi Thanh Ho[1,a*], Long Giang Bach[2,b], Dai-Viet N. Vo[3,c]

[1]Hochiminh City University of Natural Resources and Environment (HCMUNRE), Vietnam

[2]NTT Institute of Hi-Technology, Nguyen Tat Thanh University, Ho Chi Minh City, Vietnam

[3]Faculty of Chemical & Natural Resources Engineering, Universiti Malaysia Pahang, Malaysia

[a*]httvan@hcmunre.edu.vn, [b]blgiang@ntt.edu.vn, [c]vietvo@ump.edu.my

Keywords: DMFCs, $Ti_{0.7}Mo_{0.3}O_2$, PtRu/$Ti_{0.7}Mo_{0.3}O_2$, Non-carbon support

Abstract. We report the new strategy by investigating the novel $Ti_{0.7}Mo_{0.3}O_2$ material can just as easily be used as a conductive support for PtRu for DMFCs to prevent not only the carbon corrosion but also improved activity of catalyst due to some functional advantages of novel $Ti_{0.7}Mo_{0.3}O_2$ support. The $Ti_{0.7}Mo_{0.3}O_2$ nanoparticle have good crystallinity with well-defined fringes corresponding to the 3.45 Å spacing value of the {101} plane of anatase TiO_2, which were good according to the XRD pattern. The BET surface area measurements showed that the $Ti_{0.7}Mo_{0.3}O_2$ possessed 125 m^2 g^{-1} Fig. 3 shows the TEM measurement of $Ti_{0.7}Mo_{0.3}O_2$ nanoparticle and Pt/$Ti_{0.7}Mo_{0.3}O_2$, it can be observed that spherical PtRu alloy particles with an average particle size of 2-4 nm were uniformly anchored on the surface of $Ti_{0.7}Mo_{0.3}O_2$ support. More importantly, we found that there has a strong metal support interaction (SMSI) between the PtRu noble metal and the $Ti_{0.7}Mo_{0.3}O_2$ support material - resulting in facile electron donation from the $Ti_{0.7}Mo_{0.3}O_2$ support to PtRu metal with an ultimate drastic decrease in the d-band vacancy of Pt. Thus, the unique structural features of the $Ti_{0.7}Mo_{0.3}O_2$ support and the PtRu/$Ti_{0.7}Mo_{0.3}O_2$ catalyst appear to provide a suitable combination favoring that promise for the high performance of methanol oxidation, CO-tolerance in DMFCs.

Introduction

Direct methanol fuel cell (DMFC) has recently attracted much attention and has been expected as a promising candidate to compete with conventional batteries for powering portable electronic devices [1]. In DMFC, the metal catalysts for direct methanol oxidation are usually Pt or PtRu nanoparticles deposited on carbon nanosupports [2-4]. However, it is found that this system is intrinsically limited in terms of life span, and the catalytic surface area of the electrode may decrease and catalytic activity may be inactive with time due to the corrosion of carbon support and the poisoning of CO intermediate species [1, 5-7]. Hence the selection of a support for the Pt or PtRu catalyst is of critical importance to both the catalytic activity and durability [1, 8]. To address these issues, the searching of alternative catalyst support can prevent the degradation of the lifetime used in fuel cells is currently an interesting area of research and remain the challegens [8-16]. Titanium oxide (TiO_2) is one of few materials which can be stable material over the pH-potential range of interest and are structurally and chemically stable in acidic and oxidative environments [17]. Thus, TiO_2 meets the stability criterion to be used as attractive, alternative catalyst support. Unfortunately, its low electrical conductivity prevents in its use in fuel cell [15]. The conductivity of TiO_2 must be enhanced by doping, such as by cation substitution or oxygen vacancies [18]. Molybdenum oxide (MoO_x) is a conductive material that has been found with unusually characteristic about the physical and chemical properties. The nonstoichiometric lower valence molybdenum oxide contains five distinct phases, namely the Magneli phases with different compositions between MoO_3 and MoO_2. These mixed-valence molybdenum oxides have a rutile-type structure with short metal–metal bond distance along the direction of edge sharing, which accounts for their high electronic conductivity. Besides their high electronic conductivities, mixed-valence molybdenum oxides are relatively stable in acid solution and have specific catalytic activity

[19, 20]. The combination of these excellent properties of the oxides makes it is a very attractive support material for DMFCs due to the fact it would solve most of if not all of the aforementioned problems. Here, we report the new strategy by investigating the novel $Ti_{0.7}Mo_{0.3}O_2$ material can just as easily be used as a conductive support for PtRu to prevent not only the issue of carbon corrosion but also improved activity of catalyst due to some functional advantages of novel $Ti_{0.7}Mo_{0.3}O_2$ support.

Experimental

Materials. $Na_2MoO_4.2H_2O$ (99.99%), $TiCl_4$ (99.9%), $H_2PtCl_6.6H_2O$ (99.9%, 38-40% Pt), $RuCl_3.xH_2O$ (35-40% Ru), ethylene glycol (99.5%), CH_3OH (99.99%) purchased from Acros were used in the experiments. H_2SO_4 (95-97%) was from Scharlau, and Vulcan XC-72R carbon black (particle size 50 nm) was from Cabot corporation. Nafion 117 solution (5%) was obtained from Aldrich. The commercial catalysts, 20 wt% Pt/C (E-TEK), and 20 wt% Pt-10 wt% Ru/C (JM) were purchased from Alfa Aesar. Deionized water was used all through.

Synthesis of $Ti_{0.7}Mo_{0.3}O_2$ Nanoparticles. $Ti_{0.7}Mo_{0.3}O_2$ nanoparticles were prepared by a mild hydrothermal process [21]. An aqueous solution containing 12 mM Na_2MoO_4 and 28 mM $TiCl_4$ precursors solution (with Mo:Ti = 3:7 atomic ratio) was prepared. The precursor solution was then transferred to a Teflon-lined autoclave with a stainless steel shell, and heated to 200 °C at 10 °C min^{-1} in an oven. The sample was kept at 200 °C for 2 hrs in the oven and then cooled to room temperature. $Ti_{0.7}Mo_{0.3}O_2$ was washed with water and collected by centrifugation several times until the washings showed a pH 7. The precipitates were dried in a vacuum oven overnight (> 8 hrs) at room temperature for the electrochemical and textural analyses.

Preparation of 20 wt% Pt-10 wt% Ru/$Ti_{0.7}Mo_{0.3}O_2$ Nanoparticles by Microwave Enhanced Ethylene Glycol (EG) Method. The synthesis was carried out with the aid of a domestic microwave oven (LG MG-5021MW1, 300 W, 2450 MHz). Platinum (intake 20 wt%) was deposited as follows: 2.56 mL of 50 mM hexachloroplatinic acid in ethylene glycol and 0.0205 g $RuCl_3.xH_2O$ were added to 20 mL of EG to produce a yellowish solution. $Ti_{0.7}Mo_{0.3}O_2$ (0.10 g) was mixed with the solution containing hexachloroplatinic acid and ruthenium cholorua, ultrasonicated for 30 min, followed by the addition of sodium hydroxide (0.8 M) to adjust the pH to 11.0. The suspension was exposed in the middle of a microwave oven for 1 hr at 200 W (180 °C). When the reaction was complete, the sample was cooled in air, and the black precipitate was collected by repeated centrifugation and washings with acetone and deionized water. The resulting PtRu/$Ti_{0.7}Mo_{0.3}O_2$ was dried at 80 °C in a vacuum oven overnight for further use.

XRD, HRTEM, EDXA, BET Measurements. Powder X-ray diffraction (XRD) patterns of $Ti_{0.7}Mo_{0.3}O_2$, PtRu/$Ti_{0.7}Mo_{0.3}O_2$ nanocatalysts were obtained with XRD- Rigaku Dmax-B, Japan measurements using Cu K_α radiation and Ni as filter at voltage 40 kV and current 100mA. The data were collected from 20° to 90° in 2θ scale with a scan rate of 2° min^{-1}. The particle size of the as-prepared $Ti_{0.7}Mo_{0.3}O_2$ and Pt/$Ti_{0.7}Mo_{0.3}O_2$ nanoparticles was evaluated by transmission electron microscopy (TEM) using an FEI-TEM-2000 microscope operated at an accelerating voltage of 3800 kV. Specimens were prepared by ultrasonically suspending the nanoparticles in ethanol, which were then applied to a copper grid and dried in an oven.

The average composition of the $Ti_{0.7}Mo_{0.3}O_2$ support and the elemental mapping of the 30 wt% PtRu/$Ti_{0.7}Mo_{0.3}O_2$ catalyst were obtained through an energy-dispersive spectroscope (EDS-JSM 6500F, JEOL) with an accelerating voltage of 15 KV. The BET surface area of the $Ti_{0.7}Mo_{0.3}O_2$ support was obtained from N_2 adsorption isotherms at 77 K (Porous Materials, BET-202A). The material was degassed/dried at 250 °C for 3 hrs before the BET measurement in order to completely vaporize the water molecules adsorbed in the meso/micropores of the oxide. Accordingly, the BET data shown here correspond to the annealed samples.

XAS Measurements and Data Analysis. X-ray absorption spectra (XAS) were recorded at the National Synchrotron Radiation Research Centre (NSRRC) of Taiwan, Beam Line 01 C, following the procedure described in detail elsewhere [22, 23]. Experimental details, such as instrument

specifications, cell configuration, sample treatment for proper measurement, etc were the same as before. Measurements were made at room temperature with solid samples. Mo foil and MoO_2, MoO_3 were used as reference for Mo K-edge measurements, and it was a Pt foil for Pt L_{III}-edge measurements, Ru foil, RuO_2 reference for Ru K-edge. The control of parameters for EXAFS measurements, data collection modes, and calculation of errors were all done as per the guidelines set by the International XAFS Society Standards and Criteria Committee [22, 23].

Results and Discussions

X-ray diffraction (XRD) patterns of the $Ti_{0.7}Mo_{0.3}O_2$ and the $PtRu/Ti_{0.7}Mo_{0.3}O_2$ are shown in Fig. 1. The experimentally observed XRD peaks for the $Ti_{0.7}Mo_{0.3}O_2$ at 2θ positions 25.1°, 38.1°, 47.5°, 54.4°, 62.5° can be indexed to unit cell, shifted slightly from that of pure anatase-TiO_2 (JCPDS file 84-1286) due to the MoO_2 doping. No phase separation of Molybdenum oxide and Titanium oxide in $Ti_{0.7}Mo_{0.3}O_2$ can be inferred, and the entire support material is principally a single-phase solid solution. The composition of Ti, Mo binary oxide was evaluated by the EDS mapping and the EDS spectra (Fig. 2), indicating a Ti:Mo atomic ratio 68.26:31.74 (Fig. 2 (B)), which agrees closely with the expected atomic ratio of 70:30 for $Ti_{0.7}Mo_{0.3}O_2$ and the Ti and Mo is distributed uniformly. (Fig. 2 (A)).

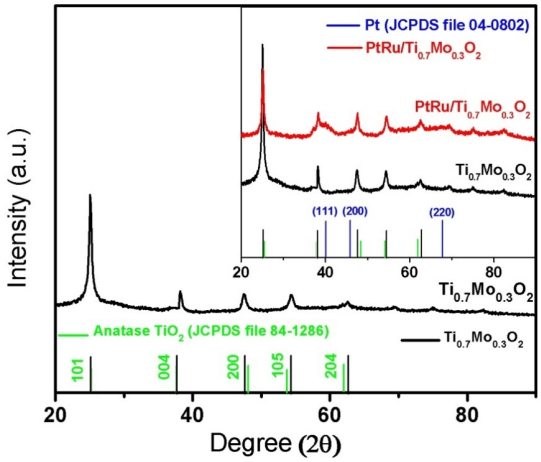

Fig. 1 X-ray diffraction pattern of $PtRu/Ti_{0.7}Mo_{0.3}O_2$ catalyst. Inset in Fig. is X-ray diffraction patterns of $PtRu/Ti_{0.7}Mo_{0.3}O_2$ and $Ti_{0.7}Mo_{0.3}O_2$.

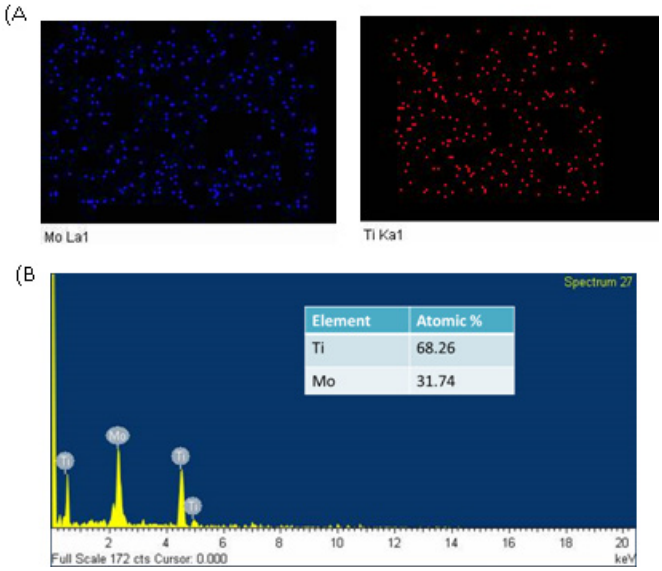

Fig. 2 (A) The EDS mapping and (B) the EDS spectra of $Ti_{0.7}Mo_{0.3}O_2$.

The $Ti_{0.7}Mo_{0.3}O_2$ nanoparticle have good crystallinity with well-defined fringes corresponding to the 3.45 Å spacing value of the {101} plane of anatase TiO_2, which were good according to the

XRD pattern. The BET surface area measurements showed that the $Ti_{0.7}Mo_{0.3}O_2$ possessed 125 $m^2 g^{-1}$ Fig. 3 shows the TEM measurement of $Ti_{0.7}Mo_{0.3}O_2$ nanoparticle and $Pt/Ti_{0.7}Mo_{0.3}O_2$, it can be observed that spherical PtRu alloy particles with an average particle size of 2-4 nm were uniformly anchored on the surface of $Ti_{0.7}Mo_{0.3}O_2$ support.

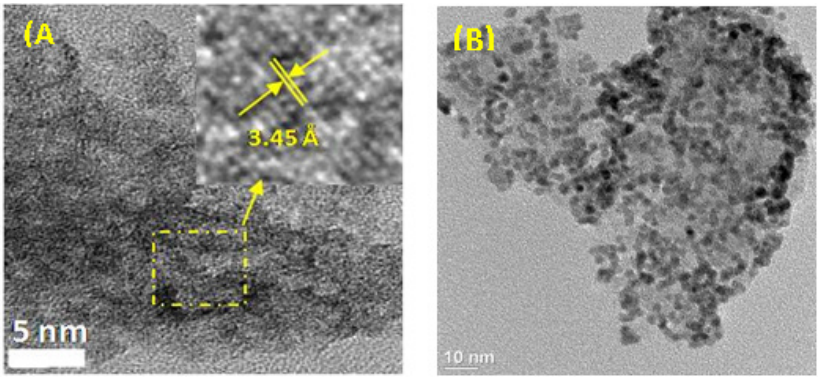

Fig. 3 (A) TEM of $Ti_{0.7}Mo_{0.3}O_2$ and (B) TEM of $PtRu/Ti_{0.7}Mo_{0.3}O_2$ catalyst.

The composition of PtRu was evalued through EDS measurement. (Fig. 4) The real amount of Pt and Ru was found 18.54 % wt. Pt: 8.92 % wt. Ru, which is closed to the 20 %wt. Pt: 10% wt. Ru.

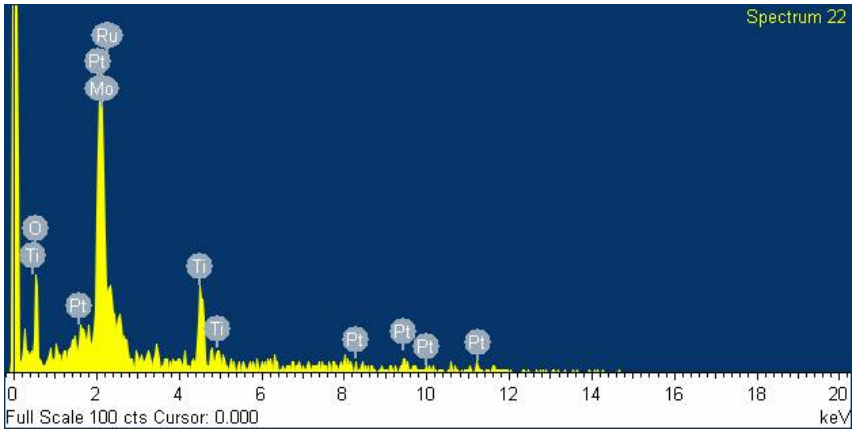

Fig. 4 The EDS spectra of $PtRu/Ti_{0.7}Mo_{0.3}O_2$ catalyst.

To probe the electronic properties of Pt in the $PtRu/Ti_{0.7}Mo_{0.3}O_2$ catalyst, the as-prepared $PtRu/Ti_{0.7}Mo_{0.3}O_2$ sample was monitored by recording XANES spectrum at the Pt L_{III}-edge (Fig. 5A). The inset in Fig. 1 shows the XRD of the $Ti_{0.7}Mo_{0.3}O_2$ and the 30 wt% $PtRu/Ti_{0.7}Mo_{0.3}O_2$ samples. The formation of crystalline PtRu nanoparticles was confirmed by the Pt(111) with an fcc structure (JCPDS file:04-0802), in addition the to the strong reflections corresponding to $Ti_{0.7}Mo_{0.3}O_2$ support. The $PtRu/Ti_{0.7}Mo_{0.3}O_2$ was further characterized by transmission electron microscopy

Similar spectra obtained for the reference Pt foil and commercial PtRu/C catalysts are also included in to this figure. It can be seen that the inset in Fig. 5(A) shows enlarged region of peaks of Pt L_{III}-edge XANES white line in which intensity of the white line, whose magnitude is a direct measure of d-band vacancy [22, 23], is of the order Pt foil > PtRu/C (JM) > $PtRu/Ti_{0.7}Mo_{0.3}O_2$ with the $PtRu/Ti_{0.7}Mo_{0.3}O_2$ showing lowest intensity. Note that the changes in white line intensity in principle could be caused by the size effect and/or the electronic effect [17, 18]. In case, the particle sizes of $PtRu/Ti_{0.7}Mo_{0.3}O_2$ and PtRu/C (JM) were similar (data not show here). Thus, the particle sizes being of similar dimension, the changes in the white line intensity for these catalyst samples are primarily a manifestation of electronic effect, inducing changes in the d-band vacancy of Pt. The decreased intensity for PtRu/C (JM) and $PtRu/Ti_{0.7}Mo_{0.3}O_2$ catalysts compared to Pt foil can be easily understood as due to an electron transfer from Ru to Pt leading to a high electron density around Pt atoms and hence a decrease in the Pt d-band vacancy [22, 23]. However, it is interesting to find that the intensity of $PtRu/Ti_{0.7}Mo_{0.3}O_2$ is much lower than PtRu/C (JM), indicating the decreased intensity of $PtRu/Ti_{0.7}Mo_{0.3}O_2$ was not only affected by the PtRu alloy structure but also

contributed by another factor. This can be assigned to arise from a different origin - a strong metal support interaction (SMSI) [19, 20] between the Pt noble metal and the $Ti_{0.7}Mo_{0.3}O_2$ support material - resulting in facile electron donation from the $Ti_{0.7}Mo_{0.3}O_2$ support to Pt metal with an ultimate drastic decrease in the d-band vacancy of Pt. In order to provide a quantitative estimate of these effects, the number of unfilled d states in the sample (h_{Ts}) was calculated, following the procedure suggested in our earlier work [22, 23]. The calculated h_{Ts} values for various samples are presented in Fig. 5B. Noticeable, the unfilled d-states (h_{Ts}) for PtRu/$Ti_{0.7}Mo_{0.3}O_2$ is obtained to 1.43, it is so worthy value, which is lower than that of commercial PtRu/C (h_{Ts} = 1.55) and Pt foil (h_{Ts} = 1.60). Due to the intensity of white line transition decrease with the decrease of d-band vacancy (h_{Ts}) [17, 18]. This noticeable feature is a good evidence to confirm the excellent strong interaction between Pt and $Ti_{0.7}Mo_{0.3}O_2$, which could also enhance the activity and stability of PtRu/$Ti_{0.7}Mo_{0.3}O_2$ catalyst compared to PtRu/C (JM), as will be shown subsequently. Thus, the unique structural features of the $Ti_{0.7}Mo_{0.3}O_2$ support and the PtRu/$Ti_{0.7}Mo_{0.3}O_2$ catalyst appear to provide a suitable combination favoring the high performance of methanol oxidation, CO-tolerance for DMFC application as discussed below.

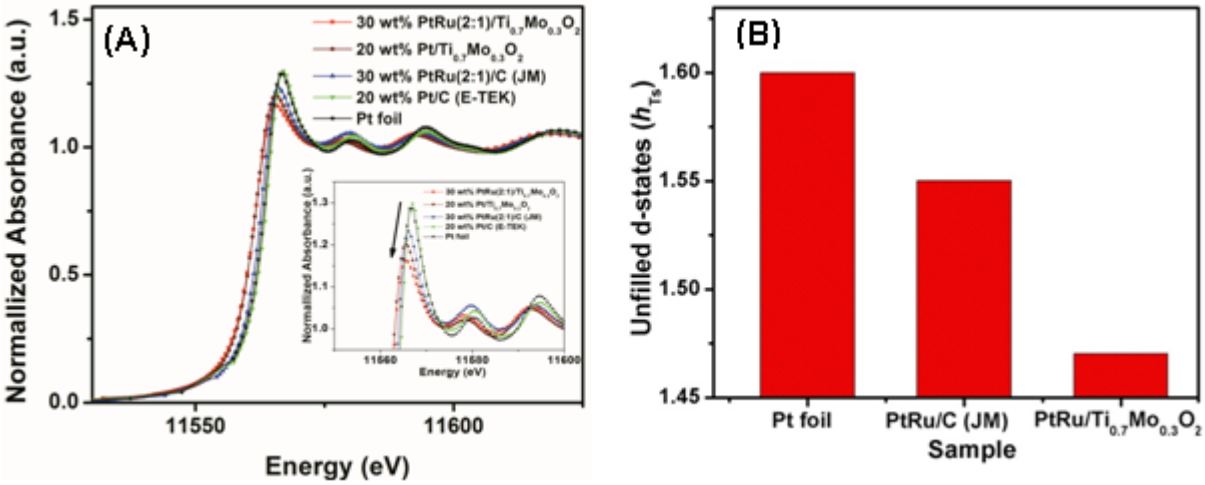

Fig. 5 (A) Pt L_{III}-edge XANES spectra, and (B) variation in unfilled d-states for Pt foil and different catalyst samples (denoted in the figure). Inset in (A) shows enlarged region of peaks of Pt L_{III}-edge XANES white line.

Conclusion

In summary, we have developed a robust non-carbon $Ti_{0.7}Mo_{0.3}O_2$ support for PtRu noble catalyst that demonstrates very high activity and durability for the MOR compared with commercial Pt/C (E-TEK) and PtRu/C (JM) catalyst. Our results suggest this enhancement is a result of both the electronic structure change of Pt upon its synergistic interaction with $Ti_{0.7}Mo_{0.3}O_2$ support and the improved mass transport kinetics of PtRu/$Ti_{0.7}Mo_{0.3}O_2$ compared to carbon support Pt or PtRu, which biases the reaction toward completion. The PtRu/$Ti_{0.7}Mo_{0.3}O_2$ also shows the high CO-tolerance due to the strong interaction between metal and support making the weak CO bond strength, thus inhibiting the self-poisoning of catalysts. Hence, above findings undoubtedly show that the suggested approach for design of the robust non-carbon catalyst is effective. The PtRu/$Ti_{0.7}Mo_{0.3}O_2$ electrocatalyst can be considered as promising candidate to improve catalytic activity and durability for DMFC. The results of this work also indicate strategies suitable for using of other dopants in TiO_2 as well as other oxide hots such for alternative catalyst support.

Acknowledgment

We gratefully thank HoChiMinh Department of Science and Technology support for this project [2015-2017].

References

[1] E. P. Lee, Z. M. Peng, W. Chen, S. Chen, H. Yang, and Y. Xia. Electrocatalytic Properties of Pt Nanowires Supported on Pt and W Gauzes, ACS Nano. 2(10) (2008) 2167–2173.

[2] T. G. Hyeon, S. J. Han, Y. E. Sung, K. W. Park and Y. W. Kim, High-Performance Direct Methanol Fuel Cell Electrodes using Solid-Phase-Synthesized Carbon Nanocoils, Angew. Chem. Int. Ed. 42 (2003) 4352-4356.

[3] R. Q. Yu, L. W. Chen, Q. P. Liu, J. Y. Lin, K. L. Tan, S. C. Ng, H. Chan, G. Q. Xu, T. S. Andyhor, Platinum Deposition on Carbon Nanotubes via Chemical Modification, Chem. Mater. 10 (1998) 718-722.

[4] S. Liao, K. A. Holmes, H. Taprailis, V. I. Birss, High Performance PtRuIr Catalysts Supported on Carbon Nanotubes for the Anodic Oxidation of Methanol, J. Am. Chem. Soc. 128 (2006) 3504.

[5] T. Y. Jeon, K. S. Lee, S. J. Yoo, Y. H. Cho, S. H. Kang and Y. E. Sung, Effect of Surface Segregation on the Methanol Oxidation Reaction in Carbon-Supported Pt−Ru Alloy Nanoparticles, Langmuir, 26 (2010) 9123-9129

[6] S. Yamazaki, M. Yao, Z. Siroma, T. Ioroi, and K. Yasuda. New-Concept CO-Tolerant Anode Catalysts Using a Rh Porphyrin-Deposited PtRu/C, J. Phys. Chem. C, 114 (2010) 21856-21860.

[7] S. Sharma, A. Ganguly, P. Papakonstantinou, X. Miao, M. Li, J. L. Hutchison, M. Delichatsios, and S. Ukleja, Rapid Microwave Synthesis of CO Tolerant Reduced Graphene Oxide-Supported Platinum Electrocatalysts for Oxidation of Methanol, J. Phys. Chem. C, 114 (2010) 19459–19466.

[8] E. Antolini, E. R. Gonzalez, Ceramic materials as supports for low-temperature fuel cell catalysts, Solid State Ionics. 180 (2009) 746–763.

[9] C. V. Subban, Q. Zhou, A. Hu, T. E. Moylan, F. T. Wagner, F. J. DiSalvo, Sol−Gel Synthesis, Electrochemical Characterization, and Stability Testing of Ti0.7W0.3O2 Nanoparticles for Catalyst Support Applications in Proton-Exchange Membrane Fuel Cells, J. Am. Chem. Soc. 132 (2010) 17531–17536.

[10] S. Y. Huang, P. Ganesan, S. Park, B. N. Popov, Development of a Titanium Dioxide-Supported Platinum Catalyst with Ultrahigh Stability for Polymer Electrolyte Membrane Fuel Cell Applications, J. Am. Chem. Soc. 131 (2009) 13898–13899.

[11] S. E. Jang, H. Kim, Effect of Water Electrolysis Catalysts on Carbon Corrosion in Polymer Electrolyte Membrane Fuel Cells, J. Am. Chem. Soc. 132 (2010) 14700-14701.

[12] K. A. N. Quoc, T. T. Huynh, V. T. T. Ho, Preparation and characterization of indium doped tin oxide (ITO) via a non-aqueous sol-gel, Molecul. Cryst. Liq. Cryst. 635 (2016) 1-8.

[13] K. A. N. Quoc, V. T. T. Ho, Preparation and Characterization of Indium Doped Tin Oxide (ITO) via a Solvothermal Method, J. Envir. Sci. Eng. B 5: 7 (2016) 379-384.

[14] K. A. N. Quoc, T. T. Huynh, V. T. T. Ho, Preparation and Characterization of Fe/Sio2 Nanoparticles Composite via Sol-Gel and Chemical Reduction Method, Int. J. Adv. Eng. Res. Sci. 3 (2016) 45-49.

[15] V. T. T. Ho, Synthesis and Characterization of PtRuMo/C Ternary Nanoelectrocatalysts for Direct Methanol Fuel Cells, Int. J. Adv. Eng. Res. Sci. 3(5) (2016) 110-114.

[16] V. T. T. Ho, T. P. Dinh, Advanced nanostructure Ti0.7In0.3O2 support enhances electron transfer to Pt: Used as high performance catalyst for oxygen reduction reaction, Molecul. Cryst. Liq. Cryst. 635 (2016) 25-31.

[17] M. Pourbaix, Atlas of Electrochemical Equilibria in Aqueous Solutions; NACE International: Houston, 1974.

[18] M. Aryanpour, R. Hoffmann, F. J. DiSalvo, Tungsten-Doped Titanium Dioxide in the Rutile Structure: Theoretical Considerations, Chem. Mater. 21 (2009) 1627-1635.

[19] H. Zhang, Y. Wang, E. R. Fachini, C. R. Cabrera, Electrochemically Codeposited Platinum/Molybdenum Oxide Electrode for Catalytic Oxidation of Methanol in Acid Solution, Electrochem. Solid-State Lett. 2 (1999) 437-439.

[20] G. Chen, Zh. Wang, D. Xia, Electrochemically codeposited palladium/molybdenum oxide electrode for electrocatalytic reductive dechlorination of 4-chlorophenol, Electrochem. Commun. 6(3) (2004) 268–272.

[21] A. Chen, P. Holt-Hindle. Platinum-Based Nanostructured Materials: Synthesis, Properties, and Applications, Chem. Rev. 110 (2010) 3767–3804.

[22] F. J. Lai, L. S. Sarma, H. L. Chou, D. G. Liu, C. A. Hsieh, J. F. Lee, B. J. Hwang, Architecture of Bimetallic PtxCo1−x Electrocatalysts for Oxygen Reduction Reaction As Investigated by X-ray Absorption Spectroscopy, J. Phys. Chem. C, 113 (2009) 12674-12681.

[23] C. C. Shih, J. R. Chang, Pt/C stabilization for catalytic wet-air oxidation: Use of grafted TiO, J. Catal. 240 (2006) 137-150.